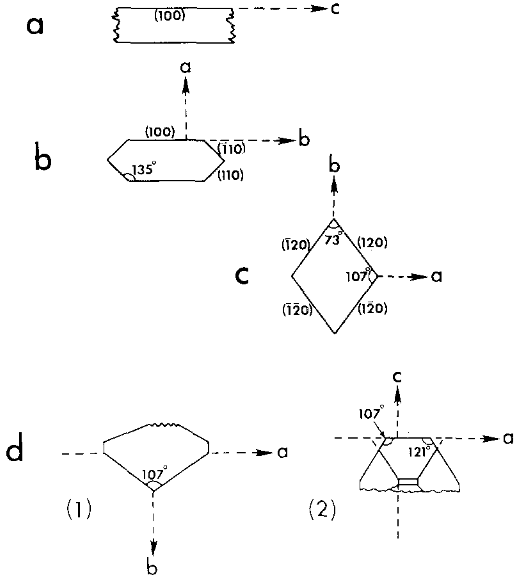

Figure 2 (a) Platelet. The major faces are (1 0 0), the long direction is the *c*-axis. (b) Tabular prism in cross-section, seen along the *c*-axis. (c) Cross-section, viewed along *c*-axis, of a rod. (d) Approximately equi-dimensional crystals (1) viewed along the *c*-axis ($a > c$). (2) viewed along the *b*-axis, indicating complex morphology.

dimensional crystals show a complex morphology having as many as twenty facets. Fig. 2 shows schematic diagrams in which some of the facets are identified.

Flux growth with relatively high concentrations of refractory oxide and, therefore, at relatively high temperatures, usually favours more equi-dimensional crystals, as has been noted with Cr_2O_3, Al_2O_3, Fe_2O_3, $NiTiO_3$, and garnets [7]. Changes in habit similar to those reported here, platy at the melt surface and more equi-dimensional within the melt, have been reported for flux grown MgO, Al_2O_3, $FeVO_4$, ZnO, CeO_2 and TiO_2 [7].

Acknowledgements

The authors thank Mr. F. R. Wondre for X-ray powder and Läue patterns, and Dr S. H. Smith and Mr B. J. Garrard for their assistance. We are grateful to Dr G. Garton for his keen interest in the work. One of us (P.N.K.) thanks the Indian U.G.C. and the British Council for supporting his visit to the United Kingdom.

References

1. E. M. LEVIN, R. S. ROTH and J. B. MARTIN, *Amer. Mineral.* **46** (1961) 1030.
2. R. W. G. WYCKOFF, "Crystal Structures" (Wiley, New York, 1964).
3. V. M. GOLDSCHMIDT and H. HAUPTMANN, *Nachr. Ges. Wiss. Göttingen, Math-Phys. Kl.*, 53 (1932).
4. B. M. WANKLYN, *J. Mater. Sci.* **8** (1973) 1055.
5. *Idem, J. Crystal Growth* **37** (1977) 334.
6. *Idem, ibid.* **43** (1978) 336.
7. *Idem,* "Crystal Growth" edited by B. R. Pamplin (Pergamon Press, Oxford, 1974).

Received 28 June
and accepted 6 September 1978.

P. N. KOTRU*
B. M. WANKLYN
Clarendon Laboratory,
University of Oxford,
Oxford, UK

---

*Present address: Department of Physics, University of Jammu, Jammu 180001, India.

Electrical conduction in 'pure' and copper-doped $KHSO_4$

Electrical conduction in hydrogen-bonded materials such as KH_2PO_4, $NH_4H_2PO_4$ (both undoped and doped with Ba^{2+}, HSO_4^- and SO_4^{2-} ions), and $(NH_4)_2SO_4:HSO_4^-$ has been demonstrated to be protonic from coulometric determination of transport numbers, electrical conductivity measurements and NMR of deuterated samples [1–5]. Quite recently, $KHSO_4$ was shown to be a protonic conductor from d.c. electrolysis experiments on Co-doped $KHSO_4$ crystals and the transport number of protons was found to be nearly unity [6]. We report in this letter, d.c. electrical conductivity results on 'pure' (undoped) and copper-doped $KHSO_4$ single crystals, in the range 50 to 180° C, the upper temperature limit being dictated by the rather low decomposition temperature (~210° C) of this hydrogen-bonded system. This study was motivated by our earlier work on the ESR of Cu^{2+} impurity in $KHSO_4$ crystals [7], where we had postulated that both K^+ and proton vacancies exist in $KHSO_4$ and that both types

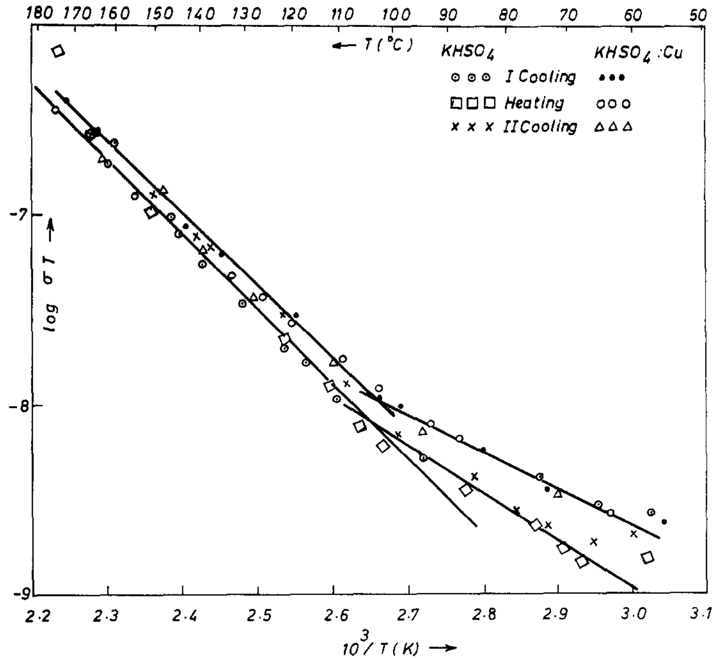

Figure 1 Electrical conductivity of $KHSO_4$ and $KHSO_4$:Cu crystals as a function of temperature.

compensate for the excess charge of the Cu(II) ion.

Single crystals of $KHSO_4$ and $KHSO_4$:Cu were grown from the appropriate saturated aqueous solutions by slow evaporation at 25° C. The materials used were "Sarabhai-Merck GR" grade $KHSO_4$ and "Extra Puriss" grade $CuSO_4 \cdot 5H_2O$. Conductivity measurements along the (0 0 1) axis of the orthorhombic crystals were carried out using a quartz-cell set-up [8], evacuated to 10^{-2} Torr, and a Keithley 610C solid-state electrometer.

Fig. 1 shows a plot of log σT versus $1000/T$, where σ is the c-axis conductivity in $(\text{ohm cm})^{-1}$ and T the temperature (K), for $KHSO_4$ and $KHSO_4$:Cu crystals. Two straight-line regions separated by a 'knee' are apparent in both cases, indicating that the same conduction mechanism is operative in both the systems. An increase in conductivity of copper-doping is also discernible. If the high-temperature region is regarded as extrinsic and the low-temperature region as structure-sensitive [9], then the addition of copper (II) has increased the number of defects already present in the undoped crystal (i.e. no new defects seem to have formed on doping).

The activation energies for the formation (E_f) and migration (E_m) of defects derived from the conductivity plots are given in Table I, which also contains data on some hydrogen-bonded crystals. On comparison, it is found that 0.52 eV in $KHSO_4$ and 0.40 eV in $KHSO_4:Cu^{2+}$, which agree well with E_m values for KH_2PO_4 and $NH_4H_2PO_4:Ba^{2+}$ respectively, represent the energy required for the migration of protons in $KHSO_4$. The common E_f (0.80 eV), which agrees well with those obtained for KH_2PO_4 and KD_2PO_4 is, in all probability, the energy of formation of a lattice defect such as a K^+ vacancy or a proton interstitial.

TABLE I Electrical conductivity data on certain hydrogen-bonded crystals

System	E_f(eV)	E_m(eV)	Reference
$KHSO_4$	0.80	0.52	Present work
$KHSO_4:Cu^{2+}$	0.80	0.40	Present work
KH_2PO_4	0.77	0.55	[1]
$KH_2PO_4:HSO_4^-$	–	0.52	[1]
KD_2PO_4	0.82	0.53	[2]
$NH_4H_2PO_4$	0.88	0.62	[3]
$NH_4H_2PO_4:Ba^{2+}$	–	0.43	[3]
$NH_4H_2PO_4:SO_4^{2-}$	–	0.47	[3]
$NH_4H_2PO_4:HSO_4^-$	–	0.54	[4]
$(NH_4)_2SO_4:HSO_4^-$	–	0.49	[4]

In $KHSO_4$, two types of HSO_4^- units exist: the dimers formed by two type I protons bridging two type I sulphate ions, and the polymeric chains (which run along the *a*-axis) formed by type II protons linking type II sulphate ions [10]. The E_f value of 0.80 eV probably represents the energy required to delink the polymeric chain, to form either free protons or relatively free HSO_4^- units which could reorient itself, resulting in proton jumps. The formation of K^+ vacancies, however, is equally probable. Thus, in the Cu^{2+}-doped $KHSO_4$ crystal, the extrinsic conduction is likely to proceed via migration of proton interstitials as well as K^+ vacancies, and, the former seem to be present in appreciable concentration even in the undoped $KHSO_4$ crystals.

Dielectric loss measurements on these crystals are expected to throw more light on the nature of the charge-compensating defects.

References

1. M. O'KEEFE and C. T. PERRINO, *J. Phys. Chem. Solids* **28** (1967) 211.
2. *Idem ibid* **28** (1967) 1086.
3. E. J. MURPHY, *J. Appl. Phys.* **35** (1964) 2609.
4. E. F. KHAIRETDINOV, V. V. BOLOYREV and A. I. BURSHTE *J. Solid State Chem.* **10** (1974) 288.
5. V. H. SCHMIDT and E. A. UEHLING, *Phys. Rev.* **266** (1962) 447.
6. M. SHARON and A. K. KALIA, *J. Chem. Phys.* **66** (1977) 305.
7. C. RAMASASTRY and C. S. SUNANDANA, *J. Magnetic Resonance* **23** (1976) 87.
8. C. S. SUNANDANA, Ph.D. Thesis, I.I.T., Madras (1975) (unpublished).
9. A. B. LIDIARD, in "Handbuch der Physik", edited by S. Flugge, Vol. 20 (Springer-Verlag, Berlin, 1957) p. 246.
10. L. H. LOOPSTRA and C. H. McGILLAVRY, *Acta Cryst.* **11** (1958) 349.

*Received 28 June
and accepted 6 September 1978.*

C. S. SUNANDANA
*Materials Science Research Centre,
Indian Institute of Technology,
Madras 600 036, India*

Pigment anti-oxidant interactions: a simple numerical analysis

In a previous publication [1] we presented experimental results of the stabilizing action of eight anti-oxidant combinations in pigmented low-density polyethylene after accelerated weathering in a Xenotest-150. Six commerical rutile pigments were used in the sample formulations. In this letter we present a simple algebraic method of assessing the polymer degradation data to estimate the extent of pigment/anti-oxidant interaction. The pigment/anti-oxidant interaction values obtained are discussed in relation to the anti-oxidant efficiency in pigmented polyethylene. Experimental details are given in the previous paper [1].

The carbonyl indices of all 63 samples after 500 h accelerated weathering are summarized in Table I. Assuming there is no interaction between anti-oxidants and pigments the effect of both components in a single system will be the sum of the pigment/polymer interaction and the polymer/anti-oxidant interaction.

The pigment interaction with the polymer PIP may be defined as:

$$\text{PIP} = \text{C.I.(usup)} - \text{C.I.(usp)} \qquad (1)$$

where C.I.(usup) = carbonyl index after *t* h irradiation of an unstabilized, unpigmented polymer film, an C.I.(usp) = carbonyl index after *t* h irradiation of an unstabilized, pigmented polymer film. When written this way, a positive value of PIP indicates a stabilizing action and conversely, a negative value indicates a sensitizing action by the pigment.

In a similar way, the anti-oxidant/polymer interaction (PIAO) can be written as:

$$\text{PIAO} = \text{C.I.(usup)} - \text{C.I.(sup)} \qquad (2)$$

where C.I.(sup) = carbonyl index after *t* h irradiation of a stabilized, unpigmented system. A positive value for PIAO indicates a stabilizing action and, conversely, a negative value indicates a sensitizing effect by the anti-oxidant.

Hence by combining Equations 1 and 2 a value for the carbonyl index after *t* h irradiation of a stabilized, pigmented system $\text{C.I.(sp)}^{\text{calc}}$ can be predicted:

$$\text{C.I.(sp)}^{\text{calc}} = 2\text{C.I.(usup)} - \text{C.I.(sup)} - \text{C.I.(usp)}. \qquad (3)$$

The ratio of this value with the actual value of C.I.(sp) will give a numerical value (AOPI) of the